Journal of Orthopaedic Translation 52 (2025) 291–300

Contents lists available at ScienceDirect

Journal of Orthopaedic Translation

journal homepage: www.journals.elsevier.com/journal-of-orthopaedic-translation

Original article

Solute transport from synovial fluid to articular cartilage and subchondral bone at different stages of osteoarthritis in a live mouse model

Mengcun Chen [a], Yanmei Yang [a], Mingshu Cui [a], Bin Wang [a,b,*]

[a] Center for Translational Medicine, Departments of Medicine and Orthopaedic Surgery, Sidney Kimmel Medical College, Thomas Jefferson University, Philadelphia, PA, 19107, United States
[b] Department of Orthopaedic Surgery, Sidney Kimmel Medical College, Thomas Jefferson University, Philadelphia, PA, 19107, United States

ARTICLE INFO

Keywords:
Osteoarthritis
Permeability
Articular cartilage
Calcified cartilage
Subchondral bone
Fluorescent dye

ABSTRACT

Objective: This study aims to (1) identify a simplified method to preserve sample integrity and maintain original fluorescence distribution; (2) assess the diffusivity of small and large molecules within articular cartilage (AC), calcified cartilage (CC), and subchondral bone (SB); and (3) investigate the changes in solute transport at various stages of osteoarthritis (OA) in a destabilization of the medial meniscus (DMM) murine model.
Methods: Fluorescent dyes of small and large molecules were injected into the knee joints of live mice. Joints were harvested and rapidly frozen immediately post-euthanasia. Optimal dye concentrations and dwelling times were determined through exploratory studies. Mice underwent either DMM or sham surgery and were evaluated at 2 and 8 weeks postoperatively. Relative fluorescence intensity was quantified within the AC, CC and SB, complemented by micro-CT, safranin O staining, and collagen II immunohistochemistry staining.
Results: The methodology successfully preserved sample integrity and original dye distribution. Fluorescent imaging revealed that small solute was mainly restricted by the tidemark, while large solute showed limited permeability in AC. Permeability of AC remained elevated in the DMM group at both time points. Increased permeability in CC and SB was observed only at 8 weeks post-DMM surgery, accompanied by reduced collagen II amount.
Conclusions: In live mice, the tidemark serves as a barrier to small molecule diffusion, while the cartilage surface restricts larger molecules; however, both structures exhibit increased permeability in OA. These findings advance the understanding of OA pathogenesis and suggest potential therapeutic targets related to cartilage permeability.
Translational Potential: The findings of this study advance the understanding of osteoarthritis pathogenesis by elucidating the role of solute transport alterations in cartilage and subchondral bone, thereby suggesting potential therapeutic targets aimed at modulating cartilage permeability to improve joint health in osteoarthritis.

1. Introduction

Osteoarthritis (OA) is a leading cause of disability and has been recognized as an organ disease that affects the entire joint [1,2]. In diarthrodial joints, articular cartilage (AC), calcified cartilage (CC), and subchondral bone (SB) are integrated into the osteochondral unit, while the synovial membrane encapsulates the joint, producing synovial fluid that lubricates and nourishes the articular surfaces, ensuring smooth and pain-free movement [3]. However, homeostasis is disrupted in OA, accompanied by inflammation mediated by various cytokines within the joint [3,4]. It is widely acknowledged that synovial fluid secreted by the synovial membrane not only plays a crucial role in maintaining joint integrity but also contributes to the initiation and progression of OA [3,5]. It has been established that tidemark acts as a barrier that interrupts the transfer of solutes between AC and CC [6,7]. Despite numerous studies focusing on cartilage transport mechanisms from the synovial fluid [1,8,9], direct evidence of the efficiency of diffusion of small and large molecules from the synovial fluid into AC and subsequently to CC and SB remains to be fully characterized.

Due to the avascular nature of cartilage, an expanding body of research is investigating the permeability and diffusivity of AC and SB in animal models [10–13]. Given its comparability in physical properties to

* Corresponding author. Center for Translational Medicine, Departments of Medicine and Orthopaedic Surgery, Sidney Kimmel Medical College, Thomas Jefferson University, Philadelphia, PA, 19107, United States.
E-mail address: bin.wang@jefferson.edu (B. Wang).

https://doi.org/10.1016/j.jot.2025.04.012
Received 5 January 2025; Received in revised form 19 March 2025; Accepted 21 April 2025

a range of nutrients and signal molecules important for chondrocyte metabolism, an *in vitro* study demonstrated that CC is permeable to small molecular solutes (~400 Da) in mature equine models [11]. However, small molecular weight solutes may not be adequately representative of larger inflammatory cytokines such as interleukin-1β (~20 kDa) and tumor necrosis factor-α (~50 kDa), which are essential factors in OA progression [2]. An *in vivo* study indicated that the diffusivity of sodium fluorescein (376 Da) is increased in OA murine models through intraperitoneal injection [13]. However, this approach did not elucidate the directionality of bone-cartilage crosstalk, as the fluorescent molecules can enter both the bloodstream and the synovial fluid. A more recent study in live mice indicated that CC could act as a barrier to the transport of Rhodamine B (467 Da) and tetramethyl-rhodamine isothiocyanate-dextran (TRITC-Dextran, 20 kDa) when the femur of mice was submerged in a Petri dish [10]. Nevertheless, this study did not encompass OA scenarios, and the fixation of the exposed femur in live mice did not accurately replicate the physiological condition of the knee joint *in vivo*. Moreover, these investigations necessitated harsh pretreatments of samples, which could be time-consuming and potentially compromise both the native structure of the tissue and the precise tracing of fluorescence, considering the high water-solubility of the fluorescent dye molecules. We recently identified the new role of calcium-binding fluorescent dye alizarin complexone in detecting permeability from articular cartilage to subchondral bone [14]. However, alizarin complexone is a small molecular solute (385 Da) and its diffusion from synovial fluid to AC cannot be visualized due to lack of calcium deposition in the articular cartilage.

Thus, the present study aims to identify a simple procedure to preserve sample integrity and maintain original fluorescence distribution; elucidate the efficiency of diffusion of both small and large molecules from synovial fluid to AC and subsequently to CC and SB; and explore the alternations of the permeability of AC and CC and SB at different stages of a mouse DMM model.

2. Material and methods

2.1. Animals

The experimental protocol was approved by the Institutional Animal Care and Use Committee of Thomas Jefferson University (Protocol No. 01830). All procedures adhered to ARRIVE guidelines and the NIH Guide for the Care and Use of Laboratory Animals. A total of 160 male C57BL/6J mice (11–12 weeks old, 25 g) were purchased from Jackson Laboratory (Bar Harbor, ME) and maintained in an AAALAC-accredited vivarium. All mice were fed standard laboratory diets (LabDiet 5001 Rodent Diet, Purina, St. Louis, MO), with food and water provided ad libitum. Prior to the initiation of the study, they underwent a one-week acclimation period.

2.2. Intra-articular injection to knee joint

Intra-articular (i.a.) injections were performed aseptically. Mice were anesthetized with 2.5 % isoflurane and 100 % oxygen. After hair removal, the injection site beneath the patella was marked using a 30 G needle attached to a syringe [15]. A sterile solution (10 μL) was administered into the right knee, after which the joint was flexed and extended three times to facilitate uniform distribution of the injected material across the entire articular surface.

2.3. Dose–response study of fluorescent dyes for diffusivity detection

A total of 27 mice were included to elucidate the optimal dosage of each dye. Rhodamine B (MW 479 Da, Sigma, Cat. No. 83689) at concentrations of 5 mM, 10 mM, 20 mM, and 40 mM, and TRITC-Dextran (MW 20 kDa, Sigma, Cat. No. 73766) at concentrations of 2.5 mM, 5 mM, 7.5 mM, and 10 mM, were i.a. administered into the right knee. Following injection, mice were housed for 30 min in the Rhodamine B group and 1 h in the TRITC-Dextran group before euthanasia. Sterile phosphate-buffered saline (PBS) was i.a. injected as a negative control. All dose–response experiments were repeated three times to ensure replicability and reliability of results.

2.4. Time-course study of fluorescent dyes for diffusivity detection

A total of 24 mice were included to investigate the optimal dwelling time of each dye. The maximal concentration, 40 mM Rhodamine B or 10 mM TRITC-Dextran, was i.a. injected in the right knee. For Rhodamine B, mice were euthanized at 7.5, 15, 30, and 60 min post-injection. For TRITC-Dextran, euthanasia was performed at 0.5, 1, 2, and 4 h post-injection. All time-course experiments were repeated three times to ensure the replicability and reliability of the results.

2.5. Cryosection processing and image visualization

Immediately after euthanasia, the knee joints were harvested and cryo-embedded in Tissue-Tek O.C.T. compound (Sakura Finetek USA Inc, Torrance, CA), followed by rapid freezing in liquid nitrogen. Ten-μm-thick coronal sections were collected using a Leica RM2155 microtome and cryo-film IIC tape (Section-Lab Co. Ltd., Hiroshima, Japan) [16]. Sections were mounted with 100 % ethanol and imaged using the EVOS™ M7000 (Thermo Fisher Scientific Inc, Waltham, MA) under both bright field and Texas Red channels to obtain bright field and fluorescence images.

2.6. Quantification of fluorescence intensity

Fluorescence intensity was quantified by two independent investigators using standardized imaging conditions, ensuring uniform brightness, contrast, and color tone. Quantification was performed (1) within the AC, extending from the articular surface to the tidemark; and (2) the region beneath the tidemark, encompassing the CC and the SB (Supplementary Fig. 1). These regions were manually delineated in bright-field images, and fluorescence intensity was measured within the corresponding areas using *ImageJ* [6]. Any images with residual meniscal tissue were excluded to avoid confounding results. Fluorescence intensity was expressed as a percentage of the maximum measurable intensity.

2.7. Destabilization of the medial meniscus (DMM) model

A total of 88 mice were randomly assigned to either the DMM group or the Sham group. The DMM model was established by transecting the medial menisco-tibial ligament (MMTL) in the right knee, as previously described [1,17], whereas the same procedure was performed without MMTL transection in sham mice. Following surgery, mice were assessed at two and eight weeks via (1) fluorescence quantification after a single intra-articular injection of fluorescent dye, administered at its optimal concentration and residence time as established by prior dose–response and time-course studies; and (2) micro-CT, histological, and immunohistochemical (IHC) analyses.

2.8. Micro-computed tomography (micro-CT) scanning

The right knees were harvested and scanned using high-resolution micro-CT (SkyScan 1275, Bruker, Kontich, Belgium). Micro-CT reconstructions and quantitative analyses were conducted using the SkyScan CT Analyzer (Version 2.3.2.0, Bruker, Kontich, Belgium), following previously described protocols [14]. Parameters such as CC thickness, SB bone volumn fraction (BV/TV) and SB thickness were analyzed.

2.9. Safranin O/Fast green staining

Knee joint samples were fixed in 4 % paraformaldehyde (PFA) for 48 h, followed by decalcification with 12 % ethylenediaminetetraacetic acid (EDTA) for two weeks. Samples were paraffin sectioned at 7 μm thickness in the coronal plane and sequentially stained with Safranin O and Fast Green solutions (0.02 % Fast Green for 5 min, 1.0 % Acetic acid for 10 s, and 0.5 % Safranin O for 5 min) [18]. Histological alternations of the medial tibial plateau (MTP) were assessed using OARSI [19], with the maximal cartilage damage score of 6.

2.10. IHC for type II collagen

Paraffin sections were subjected to immunohistochemistry for type II collagen using an anti-collagen II antibody (Abcam, Cat. No. 34712, 1:100). The streptavidin-biotin-peroxidase complex technique (Vector Laboratories, Burlingame, CA) was employed for detection, with ImmPACT DAB (Vector Laboratories) used as the chromogen. Immunolabeled sections were captured with a light microscope (BX53; Olympus, Tokyo, Japan) at 4 × or 20 × magnification. Quantification of staining intensity was performed using *ImageJ* [20].

2.11. Data analysis and statistics

The data were independently collected by two investigators and statistical analyses were conducted using GraphPad Prism, version 9. Sample sizes were determined based on previous studies [13,21,22]. Results are presented as mean ± standard deviation and bar graphs with dot plots, and n indicates the mouse number in each group. A two-tailed Student's t-test was employed to compare the outcomes between the two groups, while multiple comparisons were evaluated by one-way ANOVA with Tukey's HSD post hoc test. The significance was set at p-value less than 0.05.

3. Results

3.1. Fluorescent dye distribution in knee joints

Previous study employed 0.1 % Rhodamine B and TRITC-Dextran to assess the permeability of AC to SB by submerging the distal femoral in a petri dish [10]. However, this approach fails to accurately replicate the physiological condition of the knee joint *in vivo* and neglects the effect of joint motion on solute diffusion. In contrast, our study demonstrated that i.a. injection of fluorescent dyes in live mice resulted in even distribution and diffusion throughout the joint under physiological mechanical loading during joint motion (Fig. 1).

3.2. Cryosection collection and hydrophobic treatment of osteochondral samples

To ensure accurate fluorescence quantification, bilateral knee joint samples were harvested, and femoral and tibial segments were separated (Supplementary Fig. 2). After collection of the samples by cryofilm IIC tape, hydrophobic "rehydration" with 100 % ethanol successfully preserved the tissue structure and retained the fluorescence of the dye molecules. In contrast, samples pre-treated with 4 % PFA or 70 % ethanol failed to visualize the fluorescence for either dye (Fig. 2).

3.3. Dose–response of fluorescent dyes

The observed relative fluorescence intensity of Rhodamine B within AC was (61.4 ± 26.6)%, (76.1 ± 11.5)%, (95.5 ± 1.2)%, and (99.1 ± 0.5)% for the respective concentrations (Fig. 3A). In CC and SB (CC + SB), the relative fluorescence intensity was (5.8 ± 5.0)%, (10.6 ± 5.7)%, (13.6 ± 8.8)%, and (21.4 ± 3.6)%. These results indicated that even at the lowest concentration, the small molecular dye could reach the tidemark, leading to the selection of 40 mM Rhodamine B as the optimal concentration for following experiments.

For TRITC-Dextran, representative images at various concentrations are shown in Fig. 3B. The relative fluorescence intensity within AC was recorded as (2.6 ± 2.0)%, (3.4 ± 1.7)%, (5.9 ± 2.9)%, and (13.9 ± 4.0)%, while within CC and SB, it was (0.005 ± 0.001)%, (0.007 ± 0.003)%, (0.013 ± 0.011)%, and (0.099 ± 0.049)%. The results indicated that the synovial fluid-articular cartilage interface demonstrated restrictive effects on the large molecular solute. Based on these results, 10 mM TRITC-Dextran was selected as the optimal concentration for following experiments. In addition, no detectable fluorescence was observed in the contralateral joint (Supplementary Fig. 3).

3.4. Time-course of fluorescent dyes

Fig. 4A shows representative images of mice receiving 40 mM Rhodamine B and harvested at 7.5, 15, 30, and 60 min post-injection. The relative fluorescence intensity within AC was recorded as 97.5 ± 1.7 %, 98.9 ± 0.9 %, 97.9 ± 2.2 %, and 69.2 ± 15.6 %, respectively. For CC and SB, the relative fluorescence intensity was 12.6 ± 5.3 %, 14.8 ± 4.2 %, 21.2 ± 4.9 %, and 8.7 ± 5.1 %. The results suggest that fluorescence intensity of Rhodamine B within AC reached saturation as early as 7.5 min post-injection, remaining stable through 30 min (Fig. 4A). However, the fluorescence intensity in CC and SB peaked at 30 min,

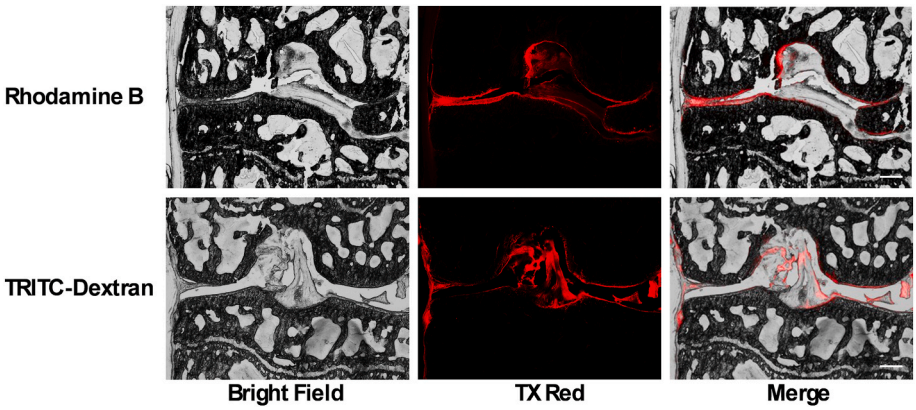

Fig. 1. Distribution of fluorescent dyes in the knee joint. Fluorescent dyes were evenly distributed in the right knee joint of normal mice following intraarticular (i.a.) injection of 5.0 mM Rhodamine B (top panel) and 5.0 mM TRITC-Dextran (bottom panel) 30 min post-injection. Fluorescence was visualized using Texas Red emission filter channels, and bright-field images were captured using the EVOS imaging system as described in the Materials and Methods section. n = 3, and representative images were shown. Scale bar: 250 μm

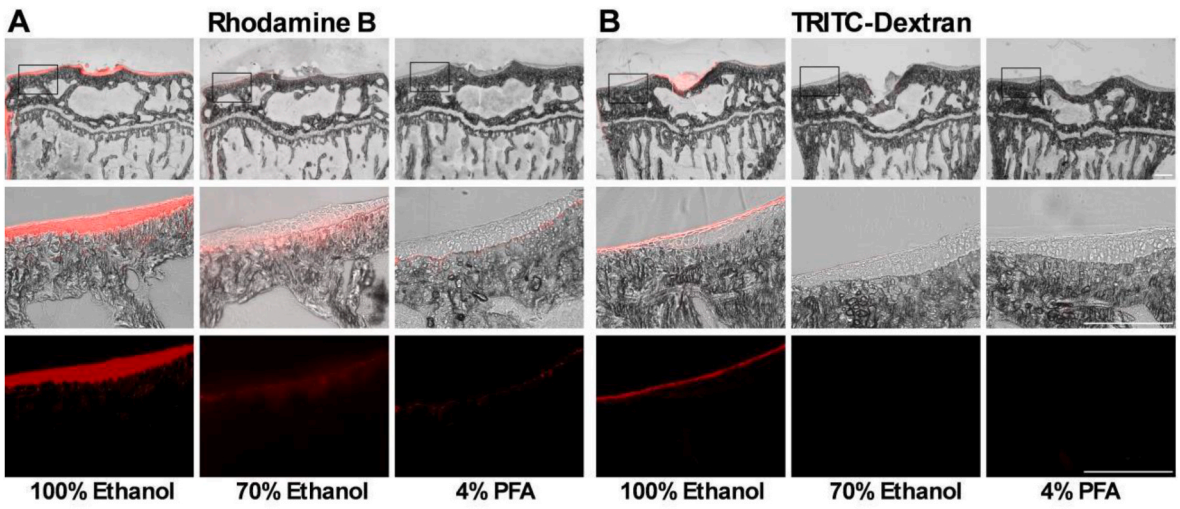

Fig. 2. High water-solubility of Rhodamine B and TRITC-Dextran. Both fluorescent dye Rhodamine B and TRITC-Dextran exhibit high water solubility, leading to dye washout when samples are fixed with aqueous solutions. To preserve the fluorescent dye, a hydrophobic "rehydration" method was employed on the tibial samples. A. Fluorescence of Rhodamine B was well-preserved and pronounced in samples processed with 100 % ethanol, but it showed substantial washout in samples rehydrated with 70 % ethanol and was nearly undetectable in those rehydrated with 4 % paraformaldehyde (PFA). B. Similarly, TRITC-Dextran fluorescence was retained and prominent in samples treated with 100 % ethanol but was almost completely lost in samples rehydrated with 70 % ethanol or 4 % PFA. Fluorescence visualization was performed using bright-field and Texas Red emission filter channels with the EVOS system, as detailed in the Materials and Methods section. Top panel: 4× merged images of bright-field and Texas Red channel; Middle panel: Magnified merged images from the boxed region in the top panel; Bottom panel: Fluorescent image of the Texas Red channel from the boxed region. n = 3, and representative images were shown. Scale bar: 250 μm

suggesting that this time point represents the optimal period for analyzing osteochondral tissue permeability.

For TRITC-Dextran, representative images of mice receiving i.a. injections of 10 mM and harvested at 0.5, 1, 2, and 4 h post-injection are shown in Fig. 4B. The relative fluorescence intensity within AC was 8.3 ± 1.9 %, 14.6 ± 2.5 %, 4.1 ± 1.2 %, and 1.4 ± 0.5 %, while within CC + SB, it was 0.044 ± 0.007 %, 0.122 ± 0.019 %, 0.011 ± 0.003 %, and 0.010 ± 0.001 %. The data indicate that, although prolonged dwelling time was in an attempt to maximize diffusion through the cartilage, the optimal dwelling time within the joint for TRITC-Dextran is 1 h post-injection.

3.5. Joint morphological alterations post-surgery

Histological analysis revealed distinct morphological changes in the MTP following DMM surgery. At 2 weeks post-surgery, no significant differences were observed between the DMM and Sham groups, with OARSI grades below 0.5 in both groups (Fig. 5A). However, at 8 weeks post-surgery, the OARSI grade of MTP in the DMM group was significantly higher (2.3 ± 0.6) compared to that in the Sham group (below 0.5) (Fig. 5B).

At 2 weeks post-surgery, no significant differences were observed in CC thickness, SB BV/TV or SB thickness between the two groups (Supplementary Fig. 4A). However, at 8 weeks, the CC thickness in the DMM group had decreased significantly compared to that in the Sham group. Additionally, SB BV/TV increased notably in the DMM group compared to that in the Sham group, while the SB thickness remained comparable between the two groups (Supplementary Fig. 4B). Collectively, our results indicate 2 weeks and 8 weeks post-DMM could be deemed as the early and intermediate to late stages of OA, respectively.

3.6. Increased permeability of AC at 2 weeks post-surgery

Representative fluorescent images of the right tibia at 2 weeks post-surgery are shown in Fig. 6. Due to the high permeability of AC to Rhodamine B, the relative fluorescence intensity within AC was nearly 100 % in both the DMM and Sham groups. The relative fluorescence intensity within CC + SB was 13.9 ± 6.3 % in the Sham group and 15.0 ± 3.5 % in the DMM group, with no significant difference observed (Fig. 6A). The relative fluorescence intensity of TRITC-Dextran within AC was significantly higher in the DMM group (n = 7, with one data point excluded due to residual meniscus) at 13.5 ± 6.8 %, compared to the Sham group at 4.7 ± 3.0 %. This finding indicates increased permeability of AC to TRITC-Dextran at 2 weeks post-DMM surgery. The fluorescence intensity of TRITC-Dextran within CC and SB remained below 0.1 % in both groups, with no significant difference (Fig. 6B). Representative images of the left tibia for Rhodamine B and TRITC-Dextran (Supplementary Fig. 5) confirm no detectable fluorescence in the contralateral joint.

3.7. Elevated permeability of both AC and CC + SB at 8 weeks post-surgery

The relative fluorescence intensity of Rhodamine B within AC was nearly 100 % in both groups. However, the relative fluorescence intensity within CC + SB significantly increased from 12.8 ± 2.1 % in the Sham group to 27.7 ± 11.4 % in the DMM group, indicating an increase in the permeability of CC + SB to Rhodamine B at this time point (Fig. 7A). The relative fluorescence intensity of TRITC-Dextran within AC was still higher in the DMM group (20.3 ± 8.5 %) than that in the Sham group (5.3 ± 3.4 %), indicating a persistent alteration in the permeability of AC to TRITC-Dextran at 8 weeks post-DMM surgery. The relative fluorescence intensity of TRITC-Dextran within CC + SB remained below 0.1 % in both groups, with no significant difference (Fig. 7B). Representative images of the left tibia for Rhodamine B and TRITC-Dextran (Supplementary Fig. 6) confirm no detectable fluorescence in the contralateral joint.

3.8. IHC staining of collagen II

IHC staining for collagen II showed no significant differences between the DMM and Sham groups at 2 weeks post-surgery (Fig. 8A). However, at 8 weeks post-surgery, collagen II staining intensity was significantly reduced in both AC and CC regions of the DMM group compared to the Sham group (Fig. 8B), suggesting extracellular matrix lesions at later stages of OA.

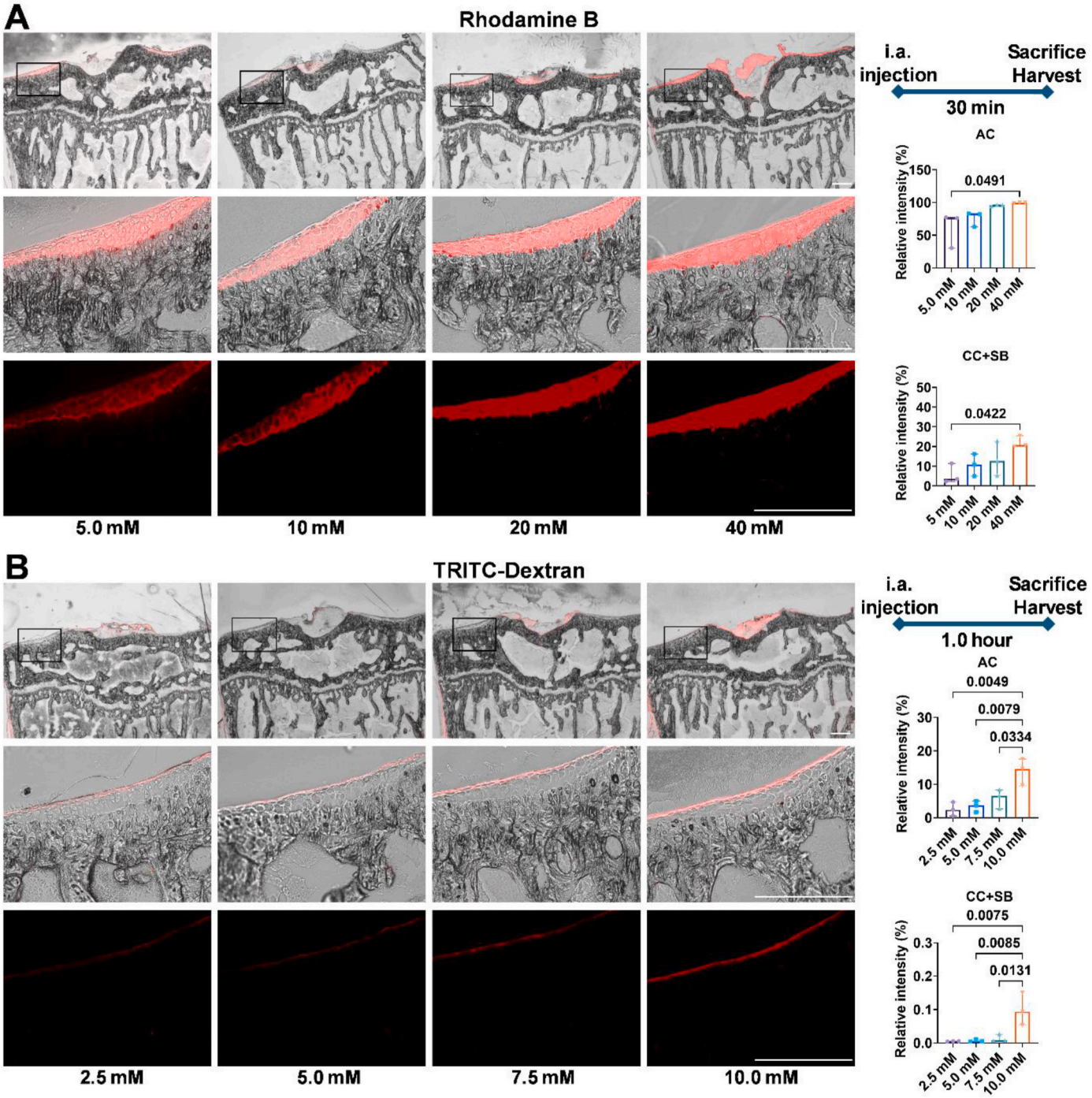

Fig. 3. Dose–response study of fluorescent dye diffusion post intra-articular injection in normal mice. A. Mice received i.a. injections of Rhodamine B at concentrations of 5 mM, 10 mM, 20 mM, and 40 mM into the right knee joint. The mice were maintained under standard housing conditions post-injection, and the knee joints were collected 30 min after the injection for analysis. The summarization of schematic timelines for the injection of Rhodamine B before the mouse sacrifice in each group are shown (right top panel). The quantified relative fluorescence intensity from three independent experiments is shown for AC (right middle panel) and CC + SB (right bottom panel). B. Mice received i.a. injections of TRITC-Dextran at concentrations of 2.5 mM, 5 mM, 7.5 mM, and 10 mM into the right knee joint. The mice were maintained under standard housing conditions postinjection, and the knee joints were collected 1.0 h after the injection for analysis. The summarization of schematic timelines for the injection of TRITC-Dextran before the mouse sacrifice in each group are shown (right top panel). The quantified relative fluorescence intensity from three independent experiments is shown for AC (right middle panel) and CC + SB (right bottom panel). Statistical significance was defined as $p < 0.05$. Scale bar: 250 μm.

4. Discussion

Increasing attention has been directed towards understanding the biochemical crosstalk within the joint [7,10–13,23]. To maximize the probability for observation of the original diffusion properties for both small and large molecules, we evaluated their diffusion within the joint *in vivo* and harvested the samples without interruptive pretreatments. Given the extremely high water-solubility of the fluorescent dye molecules, hydrophilic solvents should be avoided during sample processing [24]. Previous studies indicated that the osteochondral samples could be

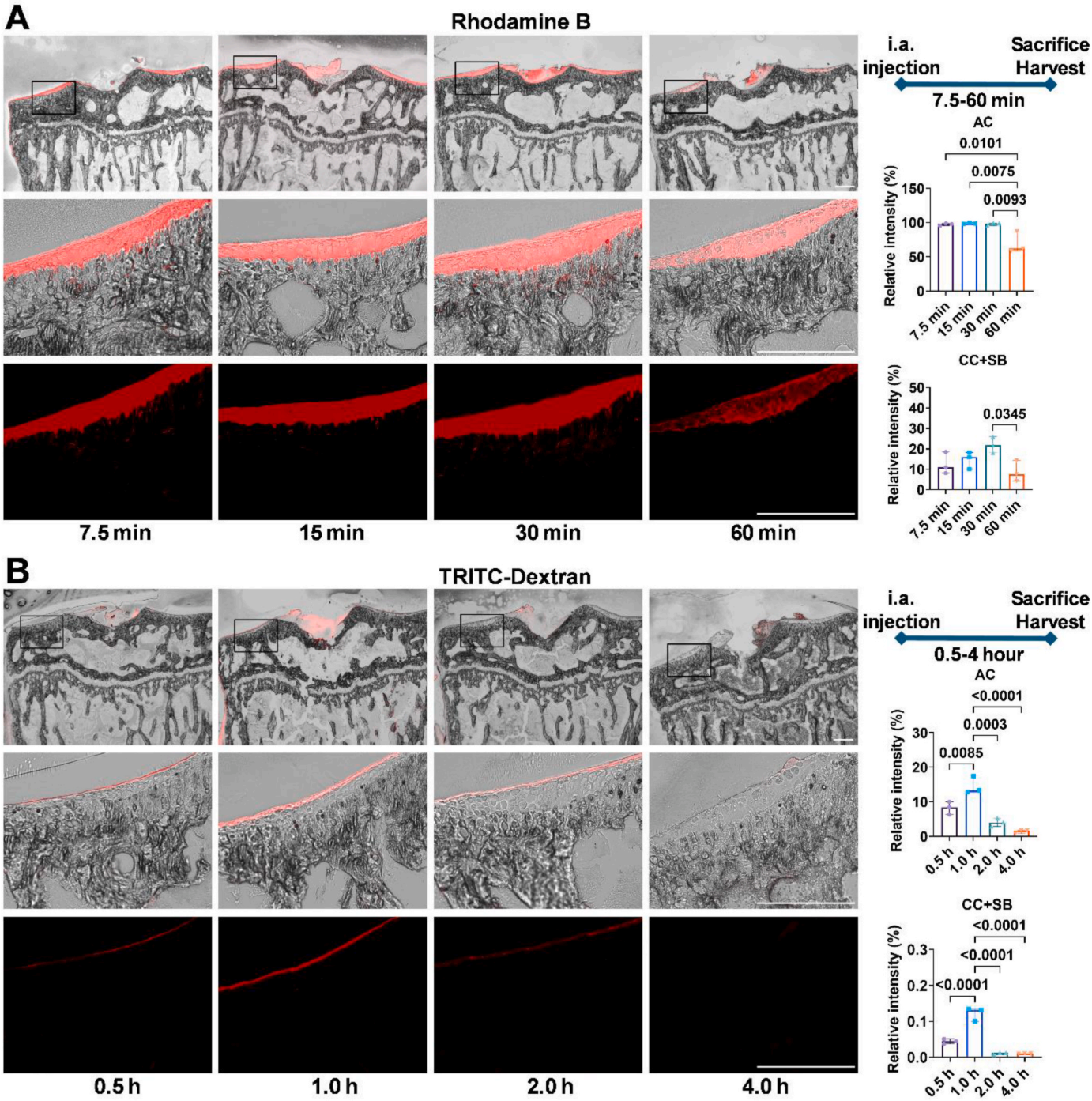

Fig. 4. Time-course study of fluorescent dye diffusion post intra-articular injection in normal mice. A. Mice received i.a. injections of 40 mM Rhodamine B into the right knee joint and were kept alive post-injection. Euthanasia was performed at 7.5, 15, 30, and 60 min post-injection for fluorescence analysis. The summarization of schematic timelines for the injection of Rhodamine B before the mouse sacrifice in each group are shown (right top panel). The quantified relative fluorescence intensity from three independent experiments is shown for AC (right middle panel) and CC + SB (right bottom panel). B. Mice received i.a. injections of 10 mM TRITC-Dextran into the right knee joint and were kept alive post-injection. Euthanasia was performed at 0.5, 1, 2, and 4 h postinjection for fluorescence analysis. The summarization of schematic timelines for the injection of TRITC-Dextran before the mouse sacrifice in each group are shown (right top panel). The quantified relative fluorescence intensity from three independent experiments is shown for AC (right middle panel) and CC + SB (right bottom panel). Statistical significance was defined as $p < 0.05$. Scale bar: 250 μm.

processed using freeze-drying and plastic embedding, though these methods were often complex and time-consuming [10,12]. In the current study, we developed a minimally invasive protocol to preserve the tissue's native structure and the original distribution of fluorescent solutes within the joint. Our findings demonstrated that both small and large molecular solutes were not fixable in either 70 % ethanol or 4 % PFA solutions, whereas 100 % ethanol was utilized to "rehydrate" and expand the cryo-sections for fluorescence analysis.

The methodology employed in the present study enabled accurate tracing of the fluorescence. In normal live mice, our findings confirmed that AC is predominantly permeable to small molecular solute, while the tidemark functions as an effective barrier, limiting their diffusion from

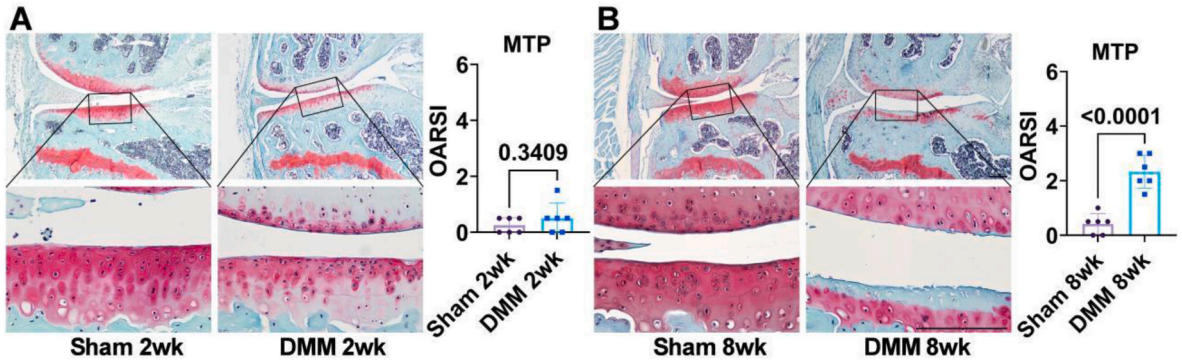

Fig. 5. Safranin-O/Fast Green staining of Sham and DMM mice. A. Two weeks post-surgery, no significant difference in OARSI grade was observed between the Sham and DMM groups. B. Eight weeks post-surgery, the OARSI grade was significantly higher in the DMM group compared to the Sham group. Images in the top panel represent 4× magnification, while the bottom panel shows a 20× magnified view of the boxed region from the top panel. n = 6/group, statistical significance was defined as $p < 0.05$. Scale bar: 125 μm.

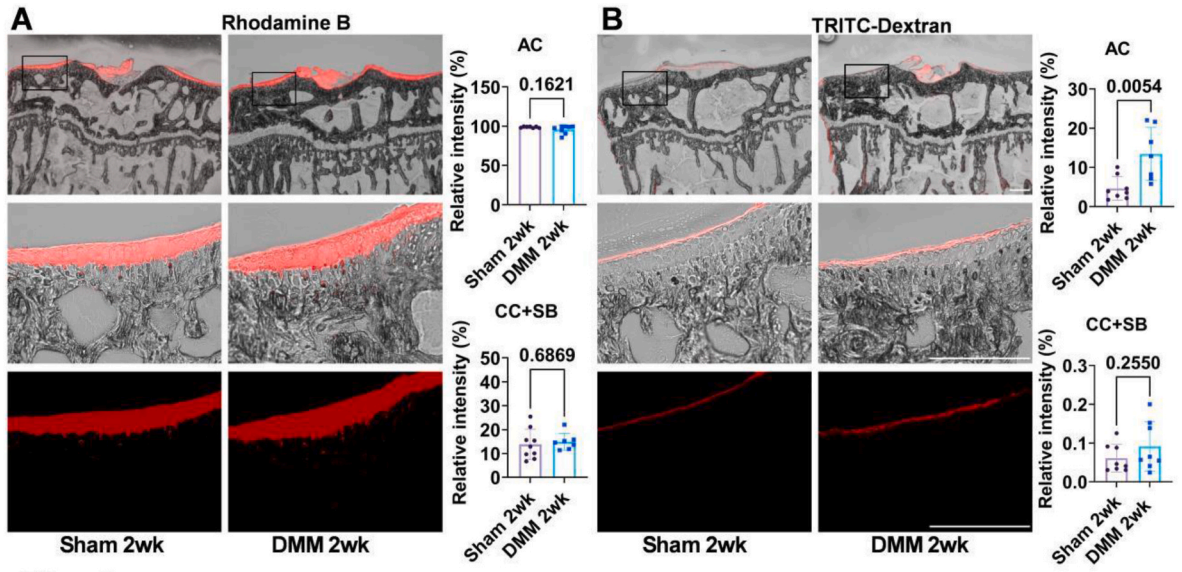

Fig. 6. Permeability of AC and CC + SB to Rhodamine B and TRITC-Dextran at two weeks postsurgery. A. Due to the high permeability of the AC to Rhodamine B, saturation was achieved within the AC in both the Sham and DMM groups. The permeability of the CC + SB to Rhodamine B was much lower than that of the AC, with no significant differences observed between the DMM and Sham groups two weeks postoperatively. B. The permeability of the AC to TRITC-Dextran increased as early as two weeks post-surgery, while the permeability of the CC + SB to TRITC-Dextran remained unchanged at this time point. n = 7–8/group, statistical significance was defined as $p < 0.05$. Scale bar: 250 μm.

AC to SB. However, we identified that AC could restrict the passage of large molecular solute, resulting in minimal fluorescence detectable at CC and SB. In the context of OA, the permeability of CC and SB for small solute remains unchanged two weeks post-surgery but increases in the eight-week DMM model, suggesting an elevated level of diffusivity from AC to SB in later stages of OA. Nevertheless, permeability changes of AC to large molecules can occur as early as two weeks post-DMM surgery and persist at eight weeks postoperatively, indicating early alterations in AC surface that precede permeability changes in the deeper zones. The diffusivity of Rhodamine B and TRITC-Dextran from synovial fluid to AC and CC + SB between the DMM and Sham mice is compared and summarized in Table 1. To our knowledge, this study is the first to employ large molecular solutes to investigate differences in AC permeability between normal and osteoarthritic mice *in vivo*.

Previous studies have suggested that CC may act as a barrier to solute transport in mature murine models [10,13], however, this barrier function deteriorates in advanced OA [23,25]. Notably, these studies using systemic administration of the fluorescent dye did not clarify the directionality of bone-cartilage interactions, as solutes could enter both the bloodstream and synovial fluid, complicating interpretation [13]. Our study, using i.a. injections, offers a more localized perspective, suggesting unidirectional diffusion from AC to SB. This is supported by the negligible influence of systemic circulation, given the solutes' high water-solubility and the small injection volume. In the present study, the fluorescence intensity of Rhodamine B reached 100 % in the AC, while the CC and SB remained permeable to small solute but exhibited significantly lower relative fluorescence, confirming the tidemark's role as a diffusion barrier for small solutes.

Multiple studies reported that the densely packed arrangement of the extracellular matrix (ECM) of the AC surface significantly hindered solute transport in the tissue, especially for larger and branched molecules [26–28]. In the present study, TRITC-Dextran was employed as a proxy for pro-inflammatory cytokines involved in the progression of OA [29,30]. Our findings demonstrate that AC exhibits substantial impermeability to TRITC-Dextran, which predominantly accumulates within its superficial layer. This provides direct evidence that AC serves as an additional hindrance, restricting the diffusion of large molecules. Moreover, the restricted diffusivity of TRITC-Dextran through AC results

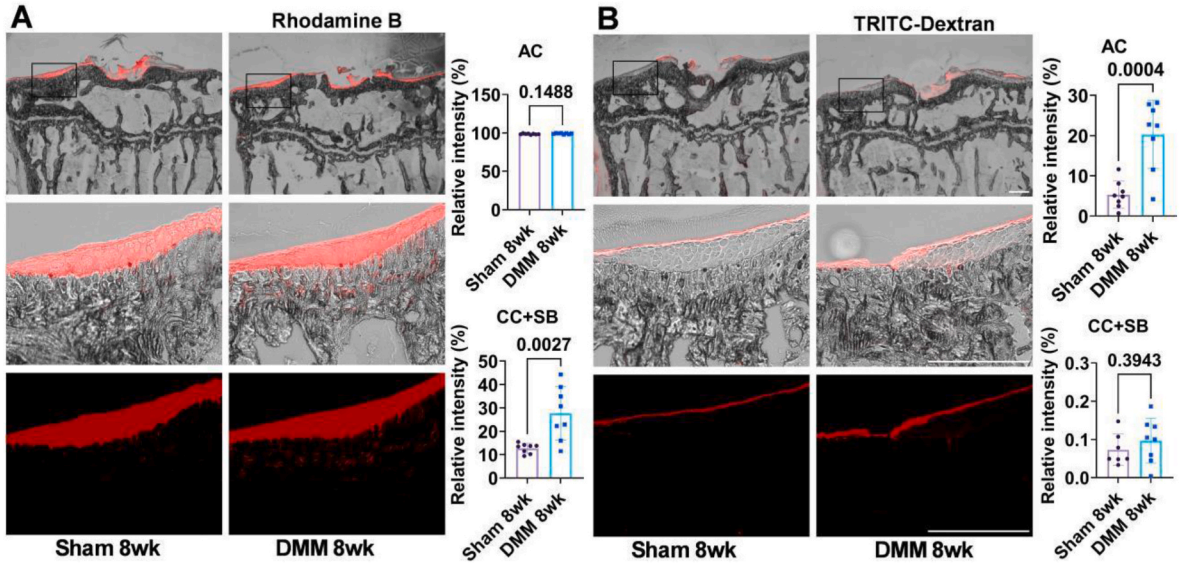

Fig. 7. Permeability of AC and CC + SB to Rhodamine B and TRITC-Dextran at eight weeks postsurgery. A. Saturation of Rhodamine B was observed within the AC in both the Sham and DMM groups. The permeability of the CC + SB to Rhodamine B was significantly higher in the DMM group compared to the Sham group eight weeks postoperatively. B. The increased permeability of the AC to TRITC-Dextran persisted eight weeks post-surgery, while the permeability of the CC + SB to TRITC-Dextran remained unchanged. n = 8/group, statistical significance was defined as $p < 0.05$. Scale bar: 250 μm.

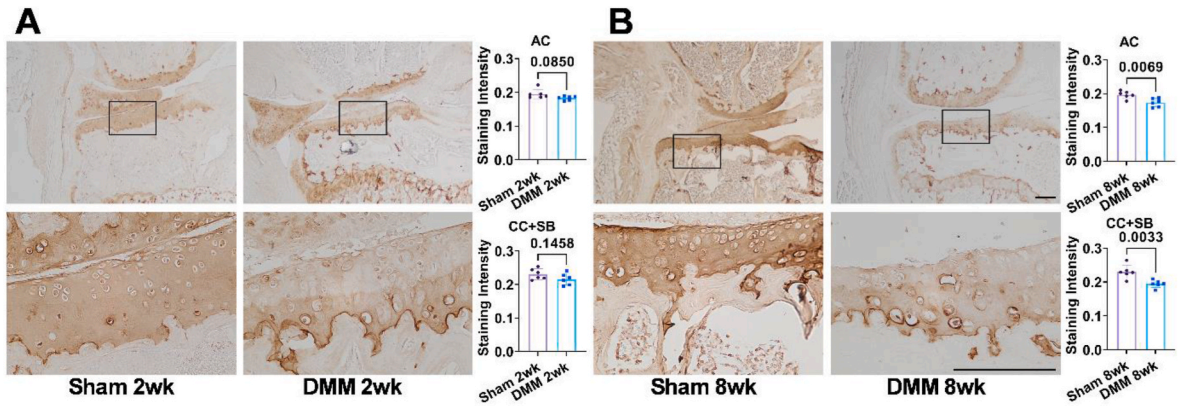

Fig. 8. Collagen II IHC staining of Sham and DMM mice. A. At two weeks post-surgery, a slight reduction in Collagen II staining intensity was observed in the AC and CC region of the DMM group, though these changes were not statistically significant. B. At eight weeks post-surgery, IHC staining intensity of Collagen II showed a significant reduction in both the AC and CC regions in the DMM group compared to the Sham group. Images in the top panel represent 4× magnification, while the bottom panel shows a 20× magnified view of the boxed region from the top panel. n = 6/group, statistical significance was defined as $p < 0.05$. Scale bar: 125 μm.

Table 1
The diffusivity of Rhodamine B and TRITC-Dextran from synovial fluid to articular cartilage and subchondral bone at various stages of DMM.

Solute transport		From synovial fluid to articular cartilage	From articular cartilage to calcified cartilage and subchondral bone
Rhodamine B (479 Da)	Sham	~100 % diffusion with no resistance	12.8–13.9 % diffusion with great resistance
	DMM 2wk	~100 % diffusion with no resistance	15.0 % diffusion with great resistance
	DMM 8wk	~100 % diffusion with no resistance	Significantly increased diffusion to 27.7 %
TRITC-Dextran (20 kDa)	Sham	4.7–5.3 % diffusion with great resistance	0.05 % diffusion with great resistance
	DMM 2wk	Significantly increased diffusion to 13.5 %	0.08 % diffusion with great resistance
	DMM 8wk	Significantly increased diffusion to 20.3 %	0.08 % diffusion with great resistance

in minimal penetration of large fluorescent solute into CC and SB. However, this observation may also be influenced by the limited time frame employed in the current study, as the diffusion of large molecular solute over an extended period might not be detectable due to potential clearance within the joint cavity at longer time points in live mice (Supplementary Fig. 7).

In the context of OA, our results showed that the fluorescence intensity of Rhodamine B saturated in AC in both Sham and DMM mice at 2 weeks and 8 weeks post-surgery. As anticipated, CC and SB permeability to small solute was unchanged between Sham and DMM groups two weeks post-surgery, supported by similar micro-CT metrics, OARSI grades, and Col II levels. At eight weeks post-surgery, a significant increase in Rhodamine B diffusion into CC and SB was observed, likely due to progressive cartilage degradation [8], evidenced by pathological alterations in these regions. Additionally, the increased leakage of interstitial fluid across tidemark and the compromised osteochondral junction in later stage OA may also contribute to the enhanced solute transport [31].

Notably, an increased tracible amount of TRITC-Dextran within AC

was observed as early as 2 weeks post-DMM surgery, despite no observable changes in joint morphology or Col II levels. The fluorescence intensity in the superficial layer of AC suggests that the observed differences may be attributed to early structural changes, such as surface corrugation, due to altered mechanical loading patterns following DMM surgery [9,32], which have been previously documented as precursors to more significant cartilage degradation in OA [33]. Particularly, the restricting effects of AC on large molecules during early-stage OA suggest that inflammatory cytokines secreted by synovial cells may not play a primary role in OA initiation. Instead, OA onset may be more closely linked to altered mechanical stimuli or stress, which activate in-situ chondrocytes or subchondral bone cells. At 8 weeks post-DMM surgery, there was a further increase in AC permeability to large solute, accompanied by increased OARSI grades and reduced Col II levels. Furthermore, some portions of the large molecular fluorescent dye were observed permeating the entire AC layer and reaching the tidemark. These suggest that the restrictive effect of AC on large solutes diminishes with the deterioration of physiological structures and reduction of key components, such as collagen II, in later stages of OA. Our observation, therefore, underscores the importance of considering the molecular weight of drugs prior to therapeutic i.a. injection, as large solutes may be impeded by the restrictive function of AC in early-stage OA.

The diffusion coefficient is a crucial parameter for predicting solute movement through cartilage and SB. It is well-established that the molecular weight of the solute is the primary factor influencing the diffusion coefficient [34]. Consistent with this principle, we observed that Rhodamine B, following i.a. injection, diffused readily into the AC without significant resistance, whereas the diffusion of TRITC-Dextran was markedly restricted. While diffusion distance typically depends on time, this assumption presupposes a constant solute concentration [35,36]. However, in live mice with intact circulation, the actual concentration of fluorescent dyes within the joint is inherently unpredictable, and fluorescence may progressively diminish due to circulatory clearance mechanisms [37,38]. Our data indicated that Rhodamine B reached its maximal fluorescence in the CC and SB at 30 min post-injection, as opposed to the expected 60 min (Fig. 4A), while TRITC-Dextran peaked in the AC at 1 h, rather than the anticipated 4 h (Fig. 4B). Prolonging the experimental time to 8 or 16 h post-injection revealed no detectable fluorescence, likely due to clearance by circulatory processes (Supplementary Fig. 7). To mitigate this issue and assess the effects of a stable solute concentration on diffusion, we i.a. injected 10 mM TRITC-Dextran into the knee joint of deceased mice 15 min post-euthanasia, eliminating blood circulation and allowing for a relatively constant dye concentration [14]. After 1 h, TRITC-Dextran diffused freely through the AC (Supplementary Fig. 8), indicating that under stable conditions, 1 h could be sufficient for its diffusion. Consequently, the fluctuation of dye concentrations in live mice impeded the accurate determination of the diffusion coefficient in cartilage and SB in this study. Future research utilizing advanced techniques will be necessary to overcome this limitation. Despite this, the use of i.a. injections remain clinically relevant, as such methods are common in therapeutic interventions.

The present study has several additional limitations. First, species-specific differences in cartilage structure, particularly the larger proportion of CC in mice, limit the generalizability of these findings to other animal models and clinical contexts. Future studies are necessary to validate the applicability of the current method to additional OA models and potential human specimens, thereby strengthening its clinical relevance and broadening its generalizability. Furthermore, the transport of solutes within cartilage involves complex reactive processes, especially for larger molecules like TRITC-Dextran, which cannot be fully explained by simple diffusion models. The transport behavior of such molecules is profoundly influenced by factors including their size, shape, and charge [39]. For instance, insulin-like growth factor I (IGF-I), a key molecule involved in cartilage maintenance, binds to multiple IGF-1-binding proteins, and the degradation of these proteins can significantly impact IGF-1 transport [40]. Finally, our study only examined the diffusion of fluorescent indicators from AC to SB; reverse diffusion from SB to AC remains unexplored, warranting further investigation into bone-cartilage crosstalk mechanisms.

5. Conclusions

The methodology employed in this study successfully preserved the native structure of osteochondral tissue samples and enabled accurate tracing of highly water-soluble fluorescent dye molecules. The results reveal that the tidemark primarily functions as a barrier to the diffusion of small molecules, whereas the interface between synovial fluid and AC appears to restrict large molecules passage but not small ones. Additionally, the observed early changes in AC permeability to large solute suggest that structural modifications may precede compositional alterations in AC. Increased permeability of AC, CC, and SB in later stage OA indicates enhanced biochemical crosstalk between AC and SB. These findings contribute to a better understanding of pathogenesis of OA and highlight the potential for targeting cartilage permeability in therapeutic interventions.

Author contributions

BW and MC conceived and designed the study. MC and BW wrote the paper., MC, YY and MC performed and analyzed the experiments. All authors edited the paper and approved the final version of the manuscript.

Disclosures

The authors have no conflicts of interest.

Data availability

The data that support the findings of this study are available on request from the corresponding author.

Funding

This work was supported, in whole or in part, by National Institutes of Health Grants R01DK119280, R01AR077666, R01AG071025, and Innovative Research Award in 2020 from the Rheumatology Research Foundation to B.W.

Appendix A. Supplementary data

Supplementary data to this article can be found online at https://doi.org/10.1016/j.jot.2025.04.012.

References

[1] Loeser RF, Goldring SR, Scanzello CR, Goldring MB. Osteoarthritis: a disease of the joint as an organ. Arthritis Rheum 2012;64(6):1697–707.
[2] Fazio A, Di Martino A, Brunello M, Traina F, Marvi MV, Mazzotti A, et al. The involvement of signaling pathways in the pathogenesis of osteoarthritis: an update. J Orthop Translat 2024;47:116–24.
[3] Lories RJ, Luyten FP. The bone-cartilage unit in osteoarthritis. Nat Rev Rheumatol 2011;7(1):43–9.
[4] Yao X, Sun K, Yu S, Luo J, Guo J, Lin J, et al. Chondrocyte ferroptosis contribute to the progression of osteoarthritis. J Orthop Translat 2021;27:33–43.
[5] DeMoya CD, Joenathan A, Lawson TB, Felson DT, Schaer TP, Bais M, et al. Advances in viscosupplementation and tribosupplementation for early-stage osteoarthritis therapy. Nat Rev Rheumatol 2024;20(7):432–51.
[6] Lyons TJ, Stoddart RW, McClure SF, McClure J. The tidemark of the chondro-osseous junction of the normal human knee joint. J Mol Histol 2005;36(3):207–15.
[7] Wang M, Tan G, Jiang H, Liu A, Wu R, Li J, et al. Molecular crosstalk between articular cartilage, meniscus, synovium, and subchondral bone in osteoarthritis. Bone Joint Res 2022;11(12):862–72.
[8] Aigner T, McKenna L. Molecular pathology and pathobiology of osteoarthritic cartilage. Cell Mol Life Sci 2002;59(1):5–18.

[9] Bader DL, Salter DM, Chowdhury TT. Biomechanical influence of cartilage homeostasis in health and disease. Arthritis 2011;2011:979032.
[10] Huang Y, Chen C, Wang F, Chen G, Cheng S, Tang Z, et al. Observation of solute transport between articular cartilage and subchondral bone in live mice. Cartilage 2021;13(2_suppl):398S–407S.
[11] Arkill KP, Winlove CP. Solute transport in the deep and calcified zones of articular cartilage. Osteoarthr Cartil 2008;16(6):708–14.
[12] Pan J, Zhou X, Li W, Novotny JE, Doty SB, Wang L. In situ measurement of transport between subchondral bone and articular cartilage. J Orthop Res 2009;27 (10):1347–52.
[13] Pan J, Wang B, Li W, Zhou X, Scherr T, Yang Y, et al. Elevated cross-talk between subchondral bone and cartilage in osteoarthritic joints. Bone 2012;51(2):212–7.
[14] Cui M, Chen M, Yang Y, Akel H, Wang B. New role of calcium-binding fluorescent dye alizarin complexone in detecting permeability from articular cartilage to subchondral bone. FASEB Bioadv 2024;6(11):539–54.
[15] Pitcher T, Sousa-Valente J, Malcangio M. The monoiodoacetate model of osteoarthritis pain in the mouse. J Vis Exp 2016;111(111):53746.
[16] Dyment NA, Jiang X, Chen L, Hong SH, Adams DJ, Ackert-Bicknell C, et al. High-throughput, multi-image cryohistology of mineralized tissues. J Vis Exp 2016;115.
[17] Glasson SS, Blanchet TJ, Morris EA. The surgical destabilization of the medial meniscus (DMM) model of osteoarthritis in the 129/SvEv mouse. Osteoarthr Cartil 2007;15(9):1061–9.
[18] Chen M, Shetye SS, Huegel J, Riggin CN, Gittings DJ, Nuss CA, et al. Biceps detachment preserves joint function in a chronic massive rotator cuff tear rat model. Am J Sports Med 2018;46(14):3486–94.
[19] Glasson SS, Chambers MG, Van Den Berg WB, Little CB. The OARSI histopathology initiative - recommendations for histological assessments of osteoarthritis in the mouse. Osteoarthr Cartil 2010;18(Suppl 3):S17–23.
[20] Riggin CN, Chen M, Gordon JA, Schultz SM, Soslowsky LJ, Khoury V. Ultrasound-guided dry needling of the healthy rat supraspinatus tendon elicits early healing without causing permanent damage. J Orthop Res 2019;37(9):2035–42.
[21] Brower TD, Akahoshi Y, Orlic P. The diffusion of dyes through articular cartilage in vivo. J Bone Joint Surg Am 1962;44(3):456–63.
[22] Arnold KM, Weaver SR, Zars EL, Tschumperlin DJ, Westendorf JJ. Inhibition of Phlpp1 preserves the mechanical integrity of articular cartilage in a murine model of post-traumatic osteoarthritis. Osteoarthr Cartil 2024;32(6):680–9.
[23] Boris Chan PM, Zhu L, Wen CY, Chiu KY. Subchondral bone proteomics in osteoarthritis: current status and perspectives. J Orthop Translat 2015;3(2):71–7.
[24] Bisballe N, Laursen BW. What is best strategy for water soluble fluorescence dyes?-A case study using long fluorescence lifetime DAOTA dyes. Chemistry 2020;26(68): 15969–76.
[25] Schultz M, Molligan J, Schon L, Zhang Z. Pathology of the calcified zone of articular cartilage in post-traumatic osteoarthritis in rat knees. PLoS One 2015;10 (3):e0120949.
[26] Bajpayee AG, Scheu M, Grodzinsky AJ, Porter RM. A rabbit model demonstrates the influence of cartilage thickness on intra-articular drug delivery and retention within cartilage. J Orthop Res 2015;33(5):660–7.
[27] Kokkonen HT, Makela J, Kulmala KA, Rieppo L, Jurvelin JS, Tiitu V, et al. Computed tomography detects changes in contrast agent diffusion after collagen cross-linking typical to natural aging of articular cartilage. Osteoarthr Cartil 2011; 19(10):1190–8.
[28] Travascio F, Valladares-Prieto S, Jackson AR. Effects of solute size and tissue composition on molecular and macromolecular diffusivity in human knee cartilage. Osteoarthr Cartil Open 2020;2(4).
[29] Leyh M, Seitz A, Durselen L, Schaumburger J, Ignatius A, Grifka J, et al. Subchondral bone influences chondrogenic differentiation and collagen production of human bone marrow-derived mesenchymal stem cells and articular chondrocytes. Arthritis Res Ther 2014;16(5):453.
[30] Sherry B, Jue DM, Zentella A, Cerami A. Characterization of high molecular weight glycosylated forms of murine tumor necrosis factor. Biochem Biophys Res Commun 1990;173(3):1072–8.
[31] Zaki S, Blaker CL, Little CB. OA foundations - experimental models of osteoarthritis. Osteoarthr Cartil 2022;30(3):357–80.
[32] Maldonado M, Nam J. The role of changes in extracellular matrix of cartilage in the presence of inflammation on the pathology of osteoarthritis. BioMed Res Int 2013; 2013:284873.
[33] Buckwalter JA, Mankin HJ, Grodzinsky AJ. Articular cartilage and osteoarthritis. Instr Course Lect 2005;54:465–80.
[34] Miyamoto S, Shimono K. Molecular modeling to estimate the diffusion coefficients of drugs and other small molecules. Molecules 2020;25(22).
[35] Lee JI, Sato M, Ushida K, Mochida J. Measurement of diffusion in articular cartilage using fluorescence correlation spectroscopy. BMC Biotechnol 2011;11:19.
[36] Leddy HA, Guilak F. Site-specific molecular diffusion in articular cartilage measured using fluorescence recovery after photobleaching. Ann Biomed Eng 2003;31(7):753–60.
[37] Evans CH, Kraus VB, Setton LA. Progress in intra-articular therapy. Nat Rev Rheumatol 2014;10(1):11–22.
[38] Mwangi TK, Berke IM, Nieves EH, Bell RD, Adams SB, Setton LA. Intra-articular clearance of labeled dextrans from naive and arthritic rat knee joints. J Control Release 2018;283:76–83.
[39] Chen Y, Lin S, Sun Y, Pan X, Xiao L, Zou L, et al. Translational potential of ginsenoside Rb1 in managing progression of osteoarthritis. J Orthop Translat 2016; 6:27–33.
[40] Zhang L, Smith DW, Gardiner BS, Grodzinsky AJ. Modeling the insulin-like growth factor system in articular cartilage. PLoS One 2013;8(6):e66870.